Numerical Investigation of the Mechanical Performance of Thoracic Aortic Aneurysm (TAA) NiTi stent

F. Nematzadeh [a,*] and H. Mostaan [a]

[a] Department of Materials Engineering, Faculty of Engineering, Arak University

Arak, P.O. Box 38156-88349, Iran

[*] Corresponding author: Tel**:** +988632625005, Mobile:+989122804069 ,Fax: +988632780801

Email address: f-nematzadeh@araku.ac.ir (F. Nematzadeh)

Abstract

Nowadays, Superelastic NiTi stent is used in Thoracic Aortic Aneurysm (TAA) because of its effects on minimizing such problems as low twistability, unsuitable dynamic behavior, and the shortage of radial mechanical strength. In our simulations, NiTi superelasticity is modeled based on Auricchio theory and Tanaka, Liang and Rogers's theory. Auricchio Model show more consistency with the experimental data than Tanaka and Liang and Rogers Models. In the present study, a Finite Element Analysis (FEA) was used to evaluate the impacts of the applied strain on the superelastic behavior of the novel design for TAA NiTi wire stent, for which axial strain (crushing) and radial strain (crimping) force are applied. The results showed that NiTi stent with 50% crimping and 90% crushing displayed the highest mechanical performance owing to suitable Chronic Outward Force (COF), appropriate Radial Resistive Force (RRF), complete mechanical hysteresis pertaining to superelastic performance, and the lesser stress and greater strain on the internal curvature of the NiTi stent. Finally, this FEM model can provide a convenient way for evaluating the biomechanical properties of TAA stents given the influences of strain applied.

Key words: crimping; crushing; NiTi stent; Thoracic Aortic Aneurysm (TAA); FEM

1. Introduction

Martensite transformation in shape memory alloys is classified as a first-order phase transformation (diffusionless and reversible) [1, 2]. Superelasticity mentions to the Stress-Induced Martensite (SIM) at temperatures higher than A_f temperature in the NiTi alloy [1]. Owing to their durability, metallic implants have been welcomed in surgical operations for a long time. Nowadays, NiTi superelastic is widely used as stents in cardiovascular treatments. Stent situation has been a key solution for cardiovascular illnesses in the previous decade [2]. Endovascular repair with stent grafts is an attractive method for solving cardiovascular diseases [3]. Recently, the use of NiTi stents has been developed for healing distal curvature or proximal descending aortic aneurysms and for supporting frame and a polyester fabric (PTFE or polyester graft materials) owing to their superelastic behavior [4]. Z-shaped stents are commonly employed for stent designing due to their well retrievability and flexibility [1, 2]. Given the extraordinary role of different parameters of the design of the stent in generating the suitable properties in the stent, analytical equations have been applied to study how geometric parameters of the stent are related to each other [1- 2, 5-6].

The first numerical study about fatigue performance of NiTi stent was introduced by Whitcher [7]. Petrini et al. found a good covenant between experimental results and numerical results during crushing test for NiTi stent [8]. Kleinstreuer et al. presented a Numerical investigation of diverse NiTi stent–graft material combinations for auxiliary abdominal aneurysm aortic (AAA) [9]. Beule et al. formulated an approach to study and to improve the mechanism of braided stents [10]. Silber et al. worked on the impact of stent geometrical features on the mechanical performance of NiTi stents [11]. Merwe et al. revealed that the use of FEA was a useful method for designing knitted NiTi meshes for approaching use as exterior vein reinforcement [12].Fortier et al. summarized the accessible

works that informations studies on biomechanical environment in healthy and diseased arteries by several analytical techniques [13].Auricchio et al. simulated novel strategy the apposition of a SAPIEN valve in a patient-specific aortic root model accounting for a number of periods characterizing the technique [14]. Pauck et al. presented a series of material tests to determine the mechanical properties of poly-L-lactic acid (PLLA); and use of the documents from these examinations in a computational study aimed at evaluating the radial behavior of polymeric stents [15].Jung et al. numerically studied the effects of geometrical structures associated on the mechanical behavior of commercial self-expandable stents and an evaluation of the resultant reactions of diverse stent patterns [16].Guerchais et al. introduced a approach for the fatigue design of balloon-expandable stents based on a micromechanical model combined with a probabilistic procedure[17].Bressloff et al. optimized Coronary Artery Stent design with the Kriging predictor functions[18].Altnji et al. urbanized numerous utilization simulations of parameterized stents by the FEM to evaluation the contact stiffness of a nitinol stent in a realistic TAA employing a Coulomb frictional model in a short-term stent fixation frame [19]. Nathan et al. revolutionized treatment of the Superficial Femoral Artery (SFA) through improvement in radial strength and incorporation of shape memory physical appearance that stimulated crush recovery [20]. Wang et al. studied RRF of vertebral body shape memory alloy stent based on design factors and biomechanical response using FEM and Response surface method (RSM) [21]. Maleckis et al. reviewed the identify challenges and provide a mechanical perspective of Femoropopliteal Artery (FPA) Nitinol stenting specific stent design and characterization of the biomechanical environment of the FPA [22].

Nonetheless, NiTi stents performance have been investigated by evenhanded a few researchers [7-29]. Numerical investigation of TAA Z-shape NiTi wire stents behavior have

not been explored yet. The present study assesses the influence of major crimping and crushing on the mechanical behavior of TAA Z-shape NiTi wire stents.

2. Research Methodology

2.1. Stent Geometry

In present work, we designed a Z-shape NiTi wire stent as shown in Fig. 1 to be used in TAA by Catia v.5 (Dassault Systèmes, USA) and were changed addicted to FEA code. Design factors of the Z-shape TAA NiTi wire stent displayed in **Fig. 1** were based on heat treatment of NiTi regarding the clinical informations derived from the literature [3-4, 30].

2.2. Material Properties and Validation of the Simulation

The present study merely compares the NiTi stents fabricated for medical applications. In our simulations, Auricchio theory is generalized in order to model NiTi superelasticity [31-37]. Factors needed in Abaqus 6.10 (Dassault Systèmes, USA) for NiTi material based on Auricchio model are listed in Table 1 [30-39]. On the others hand, NiTi superelasticity is modeled based on Tanaka, Liang and Rogers theory. EchoBio has urbanized a user material subroutine based on Tanaka and Liang and Rogers's theory [40-41]. Materials Properties used in simulation are based on Tanaka and Liang and Rogers Models as shown in Table 2 [30, 38-39]. According to Fig. 2, Table 1, and Table 2, materials properties of Auricchio theory show better consistency with the empirical information than those according to Tanaka and Liang and Rogers Models. Therefore, Auricchio model is exploited in this study for the setting up of the materials properties. The material property choice of the stents is based on the heat treatment results of the NiTi [30].

2.3. Boundary Conditions and Meshing

FE model must be replaced with actual boundary condition practical on the stent. Given the superelastic properties of NiTi stent, the displacement manner that was used was suitable. The standard tests of stent behavior were crimping and crushing .To carry out crimping test

between stent and crimper in shrinkage and extension steps, there was a surface-to-surface contact. It was supposed that the surface contact between the crimper and stent were frictionless. The crimper was subjected to a radial displacement and then, the stent restored its primary form after the displacement was removed. The diameter of the stent was decreased by 40 and 50% when the crimper was applied. To carry out crushing test, merely the contact between the stent and planes was motivated [29]. The stent was positioned under two rigid parallel planes in the Y orientation. The distance between planes was equal to the stent exterior diameter in crushing test. We supposed that the surface contact between planes and stent was frictionless. A penalty method was applied to apply resistant boundaries. At first, stent diameter was reduced by 70 and 90% in the Y direction. Since the stent geometry had axis-symmetrical natural surroundings, one-fourth of it was studied. Additionally, the temperature of environmental was assumed to be 37°C to act out the temperature of body. Hypermesh (Altair® Hypermesh® v. 6.0) is employed to mesh the models due to the meshing difficulties triggered by tiny section of the NiTi wire and comparatively difficult stents geometry. Mesh parameters of NiTi wire stent are presented in Table 3. Mesh density is 120 elements and 1010 nodes per mm^2.Because of non-convergence of the program running, we used C3D8I (incompatible mode eight-node brick) element instead of C3D8 element for solving shear locking, bending and contact of the stent. Using the elements C3D8I show good agreement with the experimentally measured responses for the Z- Shape TAA NiTi wire stent samples.

3. Results and Discussions

In the assessment of TAA NiTi stents, numerous parameters need to be controlled including superelastic hysteresis, COF, RRF, plateau stress, stress and strain. On the other hand, NiTi stents that exhibited a complete superelastic hysteresis loop, the lowest COF, the highest

RRF, higher strain and lower stress on the stent had acceptable mechanical performance [42-46]. RRF and COF are schematically illustrated in Fig. 3 as a function of the superelastic hysteresis loop. The stent is first crimped by two inflexible planes or crimpers (path a–b). Then, it is deployed so that it reaches stress stability with the blood vessel or duct at point c. The unloading curve (COF) is used to control the force in contrast to the blood vessel, and the loading curve (RRF) is used to control the force resisting deformation. Generally, stent designer's effort to design stents with as in height RRF (higher loading plateau stress) as probable and as lowest COF (lower unloading plateau stress) as probable. (a) The stents showed acceptable superelastic performance; (b) the stents ought to be in fracture safe area [47-48]. Based on the studies in this field [49-50], increasing the angle between stent parts and strain applied on the stent and increasing the inner stent diameter had suitable performance. This study shown that the increased strain applied on the NiTi stent (crimping and crushing) improved mechanical performance.

3.1. Assessing of mechanical performance of NiTi stent under crimping

Z-shape TAA NiTi wire stent designed is illustrated in Fig.1. The Maximum Von Misses Stress (MVMS) and Maximum Principal Strain (MPS) of NiTi stent resulted in 40% and 50% crimping as shown in Table 4 and Figs. 4-6. Table 4 and Figs. 4-6 summarize the computational results for stent of Fig. 1b which are crimped under performance conditions. The stents ought to perceive SIM behavior of the stress-strain curve to show appropriate superelastic behavior.The MVMS and MPS at 40% crimping shows elastic behavior. Because of the lack of superelastic behavior in these stents, they were not appropriate for the TAA application. Consequently, according to **Figs**. **4** and **6**, desired superelastic behavior was not realized with NiTi stents at 40% crimping. Comparison of results indicates that the reduction of the MVMS from 412 MPa to 401 MPa results in an minor increase in the MPS from

0.01973 to 0.02616.This increasing ratio is about 33%.With respect to the increase in crimping from 40% to 50% (indeed, higher percentage radial strain exerted on the NiTi stent), according to Table 4 and Figs. 4, 5 and 6, it is evident that MVMS on the internal curvature of NiTi stent at 40% crimping was greater than that at 50% crimping; the latter was preferred to the previous when the mechanical performance of designing these TAA NiTi stents are considered. The MPS on the internal curvature of the NiTi stent at 40% crimping was lower than that at 50% crimping; the latter possessed better dynamic motion and was more coordinated with the artery circumstance. Moreover according to Figs. 5 and 6, NiTi stent showed superelastic behavior because of the increase in crimping up to 50%. In addition, according to the assessment standards of the NiTi stent and the opinions in other studies, it was safe against mechanical loading [8, 11, 43, 49- 50]. Hence, given the mechanical standards of NiTi stents and regarding Fig. 6, the NiTi stents exhibited better mechanical performance by applying 50% crimping first owing to having superelastic behavior and then because of appropriate COF, proper RRF, high transformation strain, complete superelastic hysteresis, less stress distribution, and high strain distribution on the internal curvature of the NiTi stent. Moreover, according to Table 4, the MPS for 40% crimping is 1.973%, which is considerably lower than the crucial verge strain value limit= 8%,, while 50% crimping has a MPS of 2.616%, which is considerably lower than its crucial verge value of strain limit= 8%,. Therefore, according to the assessment standards of the NiTi stent and the observations in other studies, it was safe contrary to mechanical loading [7-9, 47-48].

3.2. Assessing of mechanical performance of NiTi stent under crushing

Z-shape TAA NiTi wire stent designed is showed in Fig.1. MVMS and MPS of NiTi induced by 70% and 90% crushing on the NiTi stent are shown in Table 5 and Figs.7, 8 and 9. Computational results for stent of Fig. 1b which are crushed under performance conditions are displayed in Table 5 and Figs. 7, 8 and 9. The paper firstly presents the results of applying 70% crushing according to standards [8] and then, presents the results of applying 90% crushing. Comparison of results reveals that the increase in the MVMS from 387.7 MPa to 443.4 MPa increases the MPS from 0.01484 to 0.03009 insignificantly. This increasing ratio is about 102%. The MVMS and MPS at 70% crushing in Table 5 and Figs.7 and 9 showed a very small hysteresis loop of superelastic behavior. As a result, this NiTi stent was not appropriate for the TAA application. With respect to the increase in crushing from 70% to 90% (indeed, higher percentage axial strain applied on the NiTi stent), the MVMS on the internal curvature of NiTi stent at 70% crushing was smaller than that at 90% crushing; the former was preferred to the latter when the mechanical properties of designing these NiTi stents for the TAA applications are taken into consideration. The MPS on the internal curvature of the NiTi stent at 70% crushing was lower than that at 90% crushing; the latter possessed superior dynamic gesture and was in better harmony with the artery circumstance. As well, the NiTi stent showed suitable superelastic behavior. It was noticeable that the NiTi stent exhibited superelastic behavior under both conditions. Therefore, according to Figs. 7 and 9 and given the NiTi stent at 70% crushing, desired superelastic behavior was not achieved because of low loop associated to superelastic behavior. However, appropriate superelastic behaviors were observed under 90% crushing. Moreover, according to evaluation standards of the NiTi stent and consistent with other studies, it was safe against mechanical loading [8, 11, 43, 49-50]. As a result, since the NiTi stents showed favorable mechanical standards and according to Fig. 9, the NiTi stents revealed better mechanical performances by applying 90% crushing owing to lower COF, higher RRF, higher transformation strain,

complete superelastic hysteresis, and higher strain on the internal curvature of the NiTi stent. Moreover, according to Table 5, the MPS for 70% crushing is 1.484%, which is considerably lower than the crucial verge strain value limit = 8%,, while 90% crushing has a MPS of 3.009%, which is considerably lower than the crucial verge strain value limit = 8%,. As a result, according to the appraisal standards of the NiTi stent and the observations in other studies, it was safe against mechanical loading [7-9, 47-48].

4. Limitations

The occurrence of the material nonlinearity, non-linear geometry, contacts, buckling, and bending make this simulation a complicated one. On the other hand, it is predicted to have self-contact during crimping and crushing process, which can by itself put extra stress on the stent. However, we can ignore these types of stresses due to the stent superelastic behavior [51]. Undoubtedly, further experiments and simulation about arteries stenosis degree are required to draw a complete end. Moreover, further experiments and simulations are needed with respect to plaque characterization, blood pressure, friction, blood vessel stenosis degree, graft and residual stresses in blood pressure.

5. Conclusion

The paper investigated the impacts of crimping and crushing on mechanical performance of Z-shape NiTi wire stent. NiTi stent with 50% crimping exhibited good mechanical performance because of the appropriate COF, proper RRF, and superelastic hysteresis complete, and lower stress distribution on the NiTi stent. Moreover, NiTi stent with 90% crushing showed desirable mechanical performance because of lower COF, higher RRF, upper transformation strain, and greater strain distribution on the NiTi stent.

Conflict of interest statement

The research conducted by the authors has been funded by the Deputy of Research and Technology of Arak University under Grant Number 92.9835(92.10.17). The authors are very grateful to Deputy of Research and Technology of Arak University.

References

[1] Duerig, T., Tolomeo, D. and Wholey, M. "An overview of superelastic stent Design", Min Invas Ther and Allied Technol, 9(3/4), pp. 235–246 (2000).

[2] Stoeckel, D., Pelton, A.R. and Duerig, T. "Self-expanding Nitinol stents: material and design considerations", Eur Radiol, 14, pp. 292–301 (2004).

[3] Matsui S.O, Terayama N, Kobayashi S. "Clinical Application of a Curved Nitinol Stent-Graft for Thoracic Aortic Aneurysms", Endovc Ther, 10, pp. 20–28 (2003).

[4] Davies J.E. "Endovascular Repair of Descending Thoracic Aortic Aneurysm: Review of Literature Thoracic", Cardiovc Surg, 21, pp.341-346(2009).

[5] Canic S, Ravi-Chandar K, Krajcer Z. "Mathematical model analysis of Wall stent and AneuRx – dynamic responses of bare-metal endoprosthesis compared with those of stent-graft" ,Tex Heart. I. J, 32, pp.502–506(2005).

[6] Patrick, B., Snowhill, B., John, L., Randall, L. and Frederick, H."Characterization of Radial Forces in Z Stents", Investigative Radiology, 36 (9), pp.521–530 (2001).

[7] Whitcher, F.D. "Simulation of in vivo loading conditions of Nitinol vascular stent structures", Comput. Struct, 64 (5-6), pp. 1005-1011 (1997).

[8] Petrini, L., Migliavacca, F., Massarotti, P., Schievano, S., Dubini, G. and Auricchio, F. "Computational studies of shape memory alloy behavior in biomedical

applications", J. Biomech. Eng, 127, pp. 716-725 (2005).

[9] Kleinstreuer, C., Li, Z,. Basciano, C., Seelecke, S. and Farber, M. "Computational mechanics of Nitinol stent grafts", J.Biomech, 41, pp. 2370–2378 (2008).

[10] Beule, M., Cauter, S., Mortier, P., Loo, D., Impec, R., Verdonck, P. and Verhegghe, B. "Virtual optimization of self-expandable braided wire stents", Med. Eng, 31, pp. 448–453 (2009).

[11] Silber, G., Alizadeh, M. and Aghajani, A. "Finite element analysis for the design of self-expandable Nitinol stent in an artery", Int. J. Energy. Tech, 2 (19), pp. 1–7 (2010).

[12] Merwe H.V.D, Reddy B. D, Zilla P. "A computational study of knitted Nitinol meshes for their prospective use as external vein reinforcement" ,J. Biomech, 41, pp. 1302–1309(2008).

[13] Fortier, A., Gullapalli, V and Mirshams, R. " Review of biomechanical studies of arteries and their effect on stent performance", IJC Heart & Vessels, 4, pp.12–18(2014).

[14] Auricchio, F., Conti, M., Morganti, S. and Reali, A. " Simulation of transcatheter aortic valve implantation: a patient-specific finite element approach", Comput Methods Biomech Biomed Engin, 17(12), pp. 1347-1357 (2014).

[15] Pauck , R.G. and Reddy, B.D. " Computational analysis of the radial mechanical performance of poly-L-lactic acid (PLLA) coronary artery stents", Med. Eng & Phy, 37, pp. 7–12 (2015).

[16] Jung, T and Kim, J. Y. " Finite element structural analysis of self-expandable stent deployment in a curved stenotic artery", J.Mech. Sci and Tech, 30 (7), pp. 3143-3149 (2016).

[17] Guerchais, R., Scalet, G., Constantinescu, A. and Auricchio, F. " Micromechanical modeling for the probabilistic failure prediction of stents in high-cycle fatigue", J.Fatigue, 87, pp. 405–417 (2016).

[18] Bressloff, N.W., Ragkousis, G and Curzen, N. " Design Optimisation of Coronary Artery Stent Systems", An.Biomed. Eng., 44, pp. 357–367 (2016).

[19] Altnji, H., Bou-Saïd,B and Walter,H." Morphological and stent design risk factors to prevent migration phenomena for a thoracic aneurysm: A numerical analysis", Med. Eng.phys, 37,pp.23-33 (2015)

[20] Nathan, A., Kobayashi, T and Giri, J. " Nitinol Self-Expanding Stents for the Superficial Femoral Artery", Interv.Card. Clin, 6, pp. 227–233 (2017).

[21] Wang, R., Zuo, H., Yang, Y.M. and Yang, B. " Finite element simulation and optimization of radial resistive force for shape memory alloy vertebral body stent ", J.Intel. Mater. Sys. Struct, 28(15), pp. 2140–2150 (2017).

[22] Maleckis, K., Anttila, E., Aylward, P. and Poulson, W. " Nitinol Stents in the Femoropopliteal Artery: A Mechanical Perspective on Material, Design, and Performance", Ann. Biomed. Eng, 46(5), pp. 684-704 (2018).

[23] Migliavacca, F., Petrini, L., Massarotti, P., Schievano, S., Auricchio, F. and Dubini, G. "Stainless and shape memory alloy coronary stents, a computational study on the interaction with the vascular wall", Biomech. Model .Mechanobiol, 2 (4), pp. 205–217 (2004).

[24] Terriault, P., Brailovski. V.and Gallo, R. "Finite element modeling of a progressively expanding shape memory stent", J.Biomech, 39 (15), pp. 2837-44 (2006).

[25] Auricchio, F., Conti, M., Beule, M., Santis, G. and Verhegghe, B. "Carotid artery stenting simulation: From patient-specific images to finite element analysis", Med. Eng.phys,33, pp. 281-289 (2011).

[26] Lorenzo V, Díaz-Lantada A, Lafont P.‟ Physical ageing of a PU-based shape memory polymer: Influence on their applicability to the development of TAA devices”, Mater & Des, 30, pp.2431-2434(2009).

[27] Elaraby A and Moratal D. ‟A generalized entropy-based two-phase threshold algorithm for noisy medical image edge detection”, Sci. Iranica D 24(6), pp. 3247-3256(2017).

[28] Zendehbudi G.R. ‟Efects of non-uniform wall properties on stress distribution in an abdominal aortic aneurysm, considering nonlinear constitutive equations”, Sci. Iranica B 21(3),pp. 620-627(2014).

[29] Nematzadeh F, Sadrnezhaad S.K. ‟Effects of material properties on mechanical performance of Nitinol stent designed for femoral artery: Finite element analysis”, Scientia Iranica, 19, pp.1564–1571(2012).

[30] Liu, X., Wang, Y., Yang, D. and Qi, M. ‟The effect of ageing treatment on shape-setting and superelasticity of a Nitinol stent”, Mater. Charact.,59, pp. 402–406 (2008).

[31] Lubliner, J. and Auricchio, F. ‟Generalized plasticity and shape memory alloy”, Int. J.Solids and Struct, 33, pp. 991–1003 (1996).

[32] Auricchio, F. and Taylor, R. ‟Shape-memory alloys: modeling and numerical simulations of the finite-strain super elastic behavior”, Compu. Meth. Appl. Mech .Eng, 143, pp. 175–94 (1996).

[33] Auricchio, F. and Taylor, R. ‟Shape-memory alloys: Modeling and numerical simulations of the finite-strain superelastic behavior”, Compu. Meth. Appl. Mech .Eng, 143 (1-2), pp. 175-194 (1997).

[34] Rebelo, N., Walker, N. and Foadian, H. ‟Simulation of implantable stents”, In: Abaqus user’s conference, 143, pp. 421–34 (2001).

[35] Conti, M., Beule, M., Mortier, P., Loo, D., Verdonck, P., Vermassen, F., Segers, P.,

Auricchio, F. and Verhegghe, B. "Nitinol Embolic Protection Filters: Design Investigation by Finite Element Analysis", J. Mater. Eng. Perform, 18, pp. 787–792 (2009).

[36] Auricchio, F., Coda, A., Reali, A. and Urbano, M. "SMA Numerical Modeling versus Experimental Results: Parameter Identification and Model Prediction Capabilities", J. Mater. Eng. Perform, 18, pp. 649–654 (2009).

[37] Arghavani, J., Auricchio, F., Naghdabadi, R. and Sohrabpour, S. "A 3-D phenomenological constitutive model for shape memory alloys under multiracial loadings", Int. J. Plasticity, 26, pp. 976-991 (2010).

[38] Khalil Allafi J, Ren X and Eggeler G. "The mechanism of multistage martensite transformation in aged Ni-rich NiTi shape memory alloys", Acta Mater, 50, pp.793-803(2002).

[39] Prince A.G, Quarini G.L, Morgan J.E. "Thermomechanical response of 50.7%Ni-Ti alloy in the pseudoelastic regime", Mater. Sci. Tech, 19, pp. 561-565(2003).

[40] Boyd J.G and Lagoudas D.C A thermodynamical constitutive model for shape memory materials. Part I. The monolithic shape memory alloy (1996).

[41] Qidwai, M.A., Lagoudas, D.C." Numerical implementation of a shape memory alloy thermomechanical constitutive model using return mapping algorithms**", Int**. J. Num. Meth. Eng, 47, pp.1123-1168**(**2000**)**.

[42] Koop, K., Lootz, D., Kranz, C., Momma, C., Becher, B. and Kieckbusch, M."Stent Material Nitinol – Determination of Characteristics and Component Simulation Using the Finite Element Method", Prog. in Biomed. Research, 6 (3), pp. 237–245 (2001).

[43] Gong, X., Duerig, T., Pelton, A., Rebelo, N. and Perry, K."Finite element analysis and experimental evaluation of superelastic Nitinol stents", In Proceedings of the

International Conference on Shape Memory and Superelastic Technology Conference – SMST (2003).

[44] Gideon, V., Kumar, P. and Mathew, L."Finite Element Analysis of the Mechanical Performance of Aortic Valve Stent Designs", Trends Biomater.Artif.Organs, 23 (1), pp. 16-20 (2009).

[45] Salaheldin, M., Zilla, S. and Franz, T. "A. Computational Study of Structural Designs for a Small-Diameter Composite Vascular Graft Promoting Tissue Regeneration", Cardiovascular Eng. Tech, 1 (4), pp. 269–281 (2010).

[46] Auricchio, F., Conti, M., Morganti, S. and Reali, A. "Shape Memory Alloy: from Constitutive Modeling to Finite Element Analysis of Stent Deployment", CMES, 57 (3), pp. 225-243 (2010).

[47] Pelton, A.R., Schroeder, V., Mitchell, M., Gong, X., Barneya, M., Robertson, S. "Fatigue and durability of Nitinol stents", J. Mech. Behav.Biomed. Mater, 1, pp. 153–164 (2008).

[48] Santillo, M. "Fracture and crack propagation study of a Superficial Femoral Artery Nitinol stent", Ms Thesis University of Pavia, Italy (2008).

[49] Wang, R., Ravi-Chandar, K. "Mechanical response of a metallic aortic stent – Part I: Pressure diameter relationship", J. Appl.Mech, 71,pp. 697–705(2004a).

[50] Wang, R., Ravi-Chandar, K, " Mechanical response of a metallic aortic stent – Part II: A beam on elastic foundation model", J. Appl.Mech, 71, pp.706–712 (2004b).

[51] Wu, W., Qi, M., Liu, X., Yang, D. and Wang, W. "Delivery and release of Nitinol stent in carotid artery and their interactions: a finite element analysis", J.Biomech, 40 (13), pp. 3034-40 (2007).

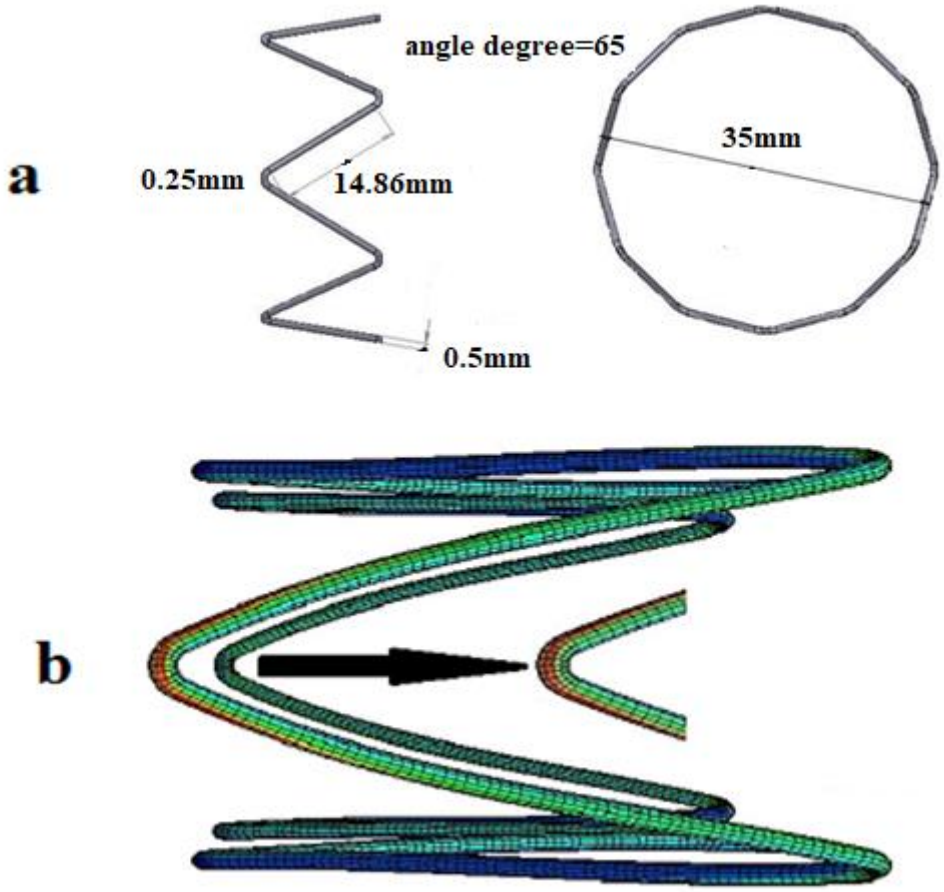

Fig. 1. Designing Z-shaped NiTi wire stent for TAA application based on material properties and clinical reports [3-4, 20].: (a) geometric details, (b) exact position of the stent where computational calculations have been done. (Unit of length is mm)

Table 1. Material properties of the TAA NiTi stent based on Auricchio model [20-29].

Symbol	Description	Unit	value
$\mathbf{E_A}$	Austenite elasticity	**MPa**	20700
$\boldsymbol{\nu_A}$	Austenite Poisson's ratio		0.33
$\mathbf{E_M}$	Martensite elasticity	**MPa**	11700
$\boldsymbol{\nu_M}$	Martensite Poisson's ratio	-	0.33
$\boldsymbol{\varepsilon^L}$	Transformation strain	-	0.055
$(\delta\sigma/\delta T)_L$	stress/temperature ratio during loading	**MPa T^{-1}**	5.32
σ_L^S	Start of transformation loading	**MPa**	344
σ_L^E	End of transformation loading	**MPa**	363
T_0	Reference temperature	$^{\circ}C$	37
$(\delta\sigma/\delta T)_U$	stress/temperature ratio during unloading	**MPa T^{-1}**	5.32
σ_U^S	Start of transformation unloading	**MPa**	58
σ_U^E	End of transformation unloading	**MPa**	42
σ_{CL}^S	Start of transformation stress in compression	**MPa**	0
ε_V^L	Volumetric transformation strain	-	0.055
$\varepsilon_{\max}$	Strain limit		0.08
A_f	Austenite finish temperature	$^{\circ}C$	24

Table 2. Material properties of the TAA NiTi stent based on Tanaka and Liang and Rogers Models [20, 28-29, 30-31].

Symbol	Description	Unit	value
$\mathbf{E_A}$	Austenite elasticity	**MPa**	20700
v	Poisson's ratio		0.33
$\mathbf{E_M}$	Martensite elasticity	**MPa**	11700
$\boldsymbol{\rho}$	Density	$\mathbf{kg/m^3}$	6450
$\mathbf{K_A}$	Thermal Conductivity	**w/(m.K)**	18
$\mathbf{C_A}$	Austenite Specific Heat	**J/(kg.K)**	320
$\boldsymbol{\alpha_A}$	Austenite Thermal Expansion Coeff	**1/K**	11×10^{-6}
$\boldsymbol{\alpha_M}$	Martensite Thermal Expansion Coeff	**1/K**	6.6×10^{-6}
$\boldsymbol{\rho s_A}$	Stress Influence Coefficient for Austenite	**MPa/K**	-0.1705×10^{6}
$\boldsymbol{\rho s_M}$	Stress Influence Coefficient for Martensite	**MPa/K**	-0.905×10^{6}
$\mathbf{M_f}$	Martensite Finish Temperature	**K**	287
$\mathbf{M_s}$	Martensite Start Temperature	**K**	291
$\boldsymbol{A_s}$	Austenite Start Temperature	**K**	293
$\boldsymbol{A_f}$	Austenite Finish Temperature	**K**	297

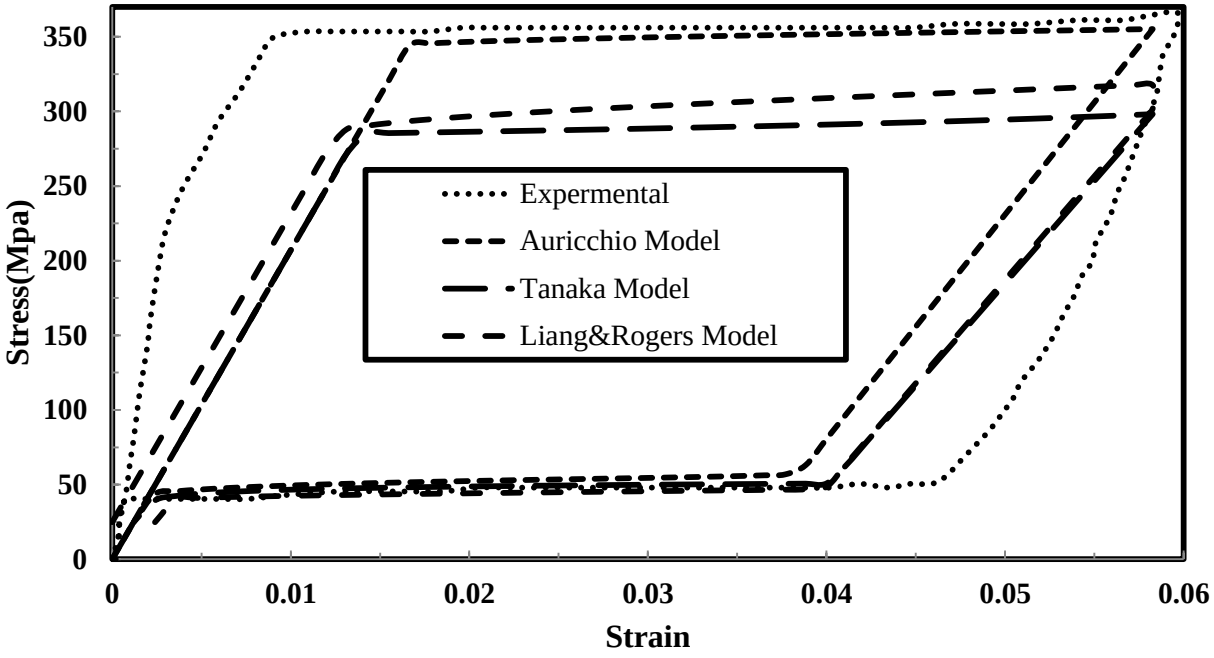

Fig. 2. Comparison of Auricchio and Tanaka and Liang and Rogers Models calculations with empirical data achieved for NiTi sample demonstrated in **Tables 1** and **2**.

Table 3. Mesh parameters of TAA NiTi stent during crimping and crushing

Material	Element type	Number of elements	Number of nodes
Stent with 6 bends	C3D8I	14400	18900
Crimper	SFM3D4	206275	207390
Stent with 6 bends	C3D8I	14400	18974
Rigid Plane	R3D4	**1120**	11502

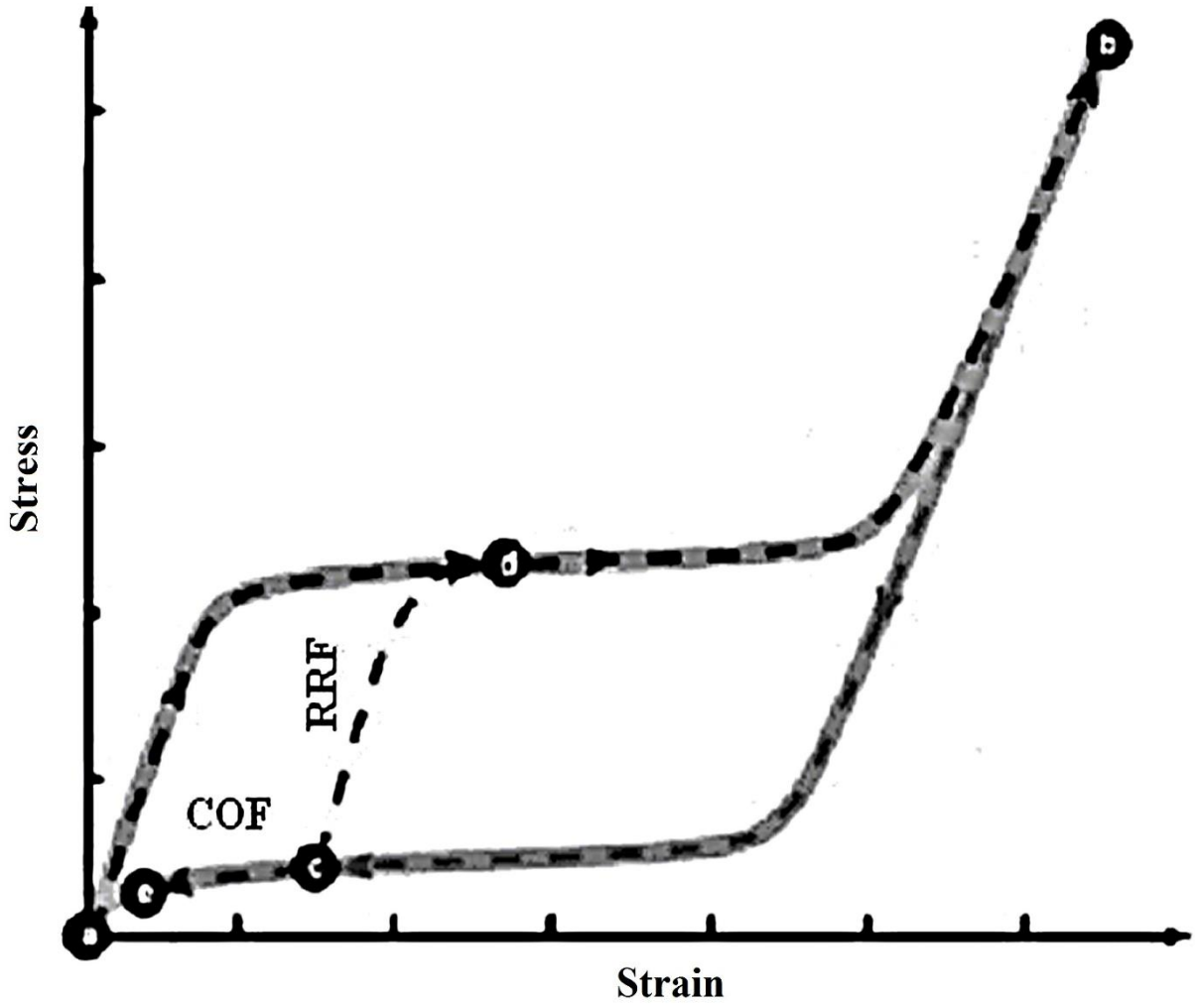

Fig. 3. Superelastic hysteresis loop related to **RRF** and **COF**

Table 4. Stress and strain results of the TAA stent under crimping

Stent Performance	MVMS (MPa)	MPS	Strain limit
40% crimping	412	0.01973	0.08
50% crimping	401.8	0.02616	0.08

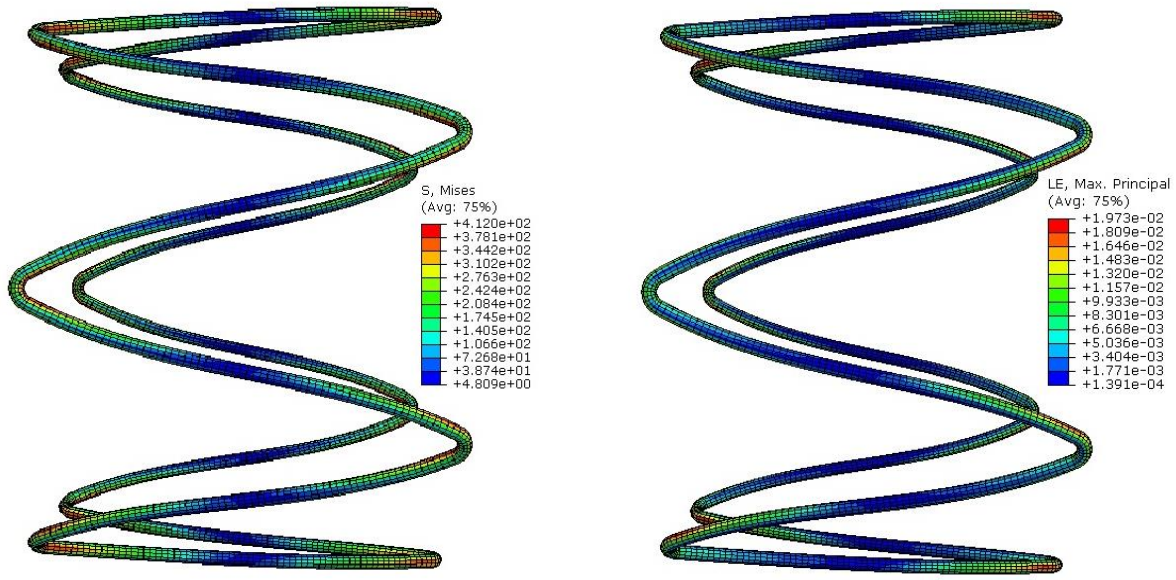

(a) (b)

Fig. 4. Results of 40% crimping of the TAA stent shown in **Fig. 1**: (a) MVMS, (b) MPS

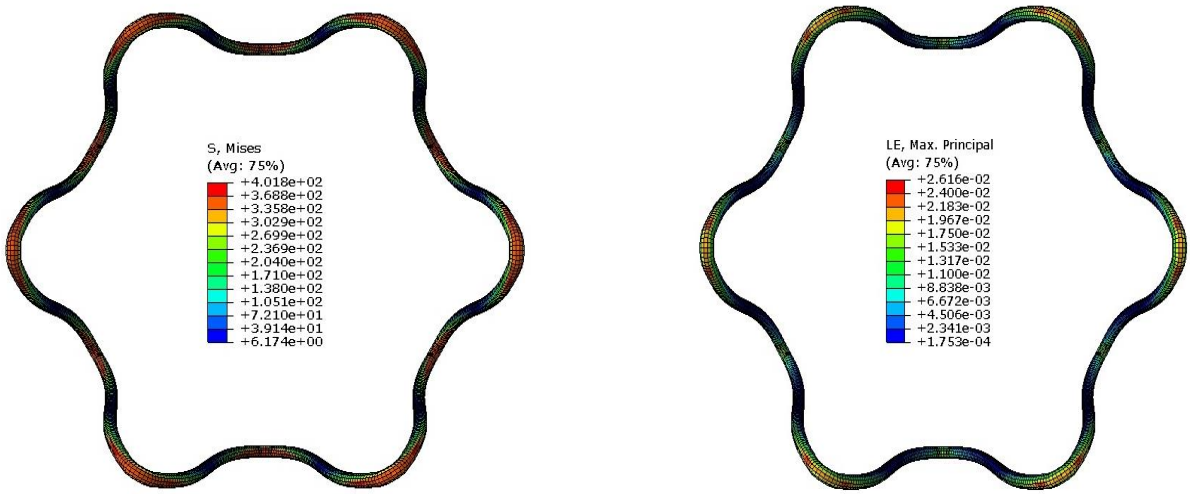

(a) (b)

Fig. 5. Results of 50% crimping of the TAA stent shown in **Fig. 1**: (a) MVMS, (b) MPS

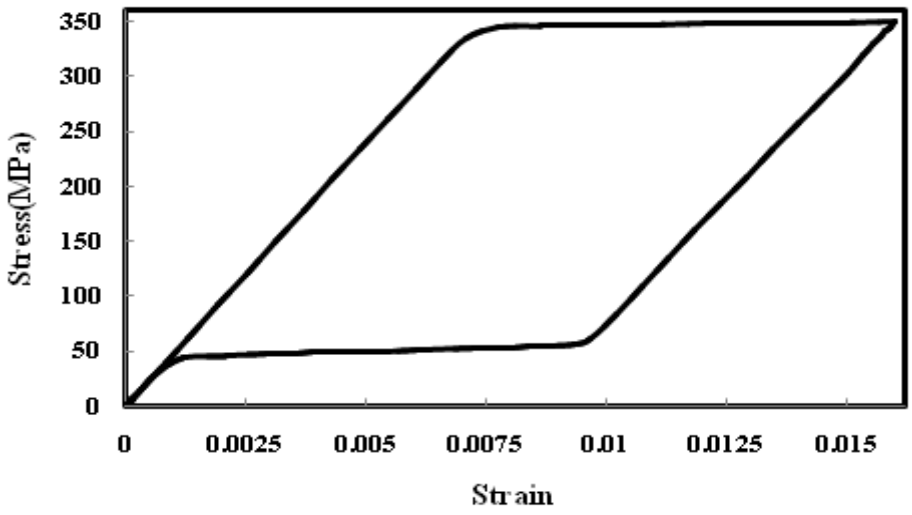

Fig. 6. Results of Superelasticity behavior plotted in 50% crimping on NiTi stent shown in **Fig. 1** (NiTi stent did not show superelasticity behavior in 40% crimping).

Table 5. Stress and strain results of the TAA stent under crushing

Stent performance	**MVMS** (MPa)	**MPS**	**Strain limit**
70% crushing	388	0.01484	0.08
90% crushing	443	0.03009	0.08

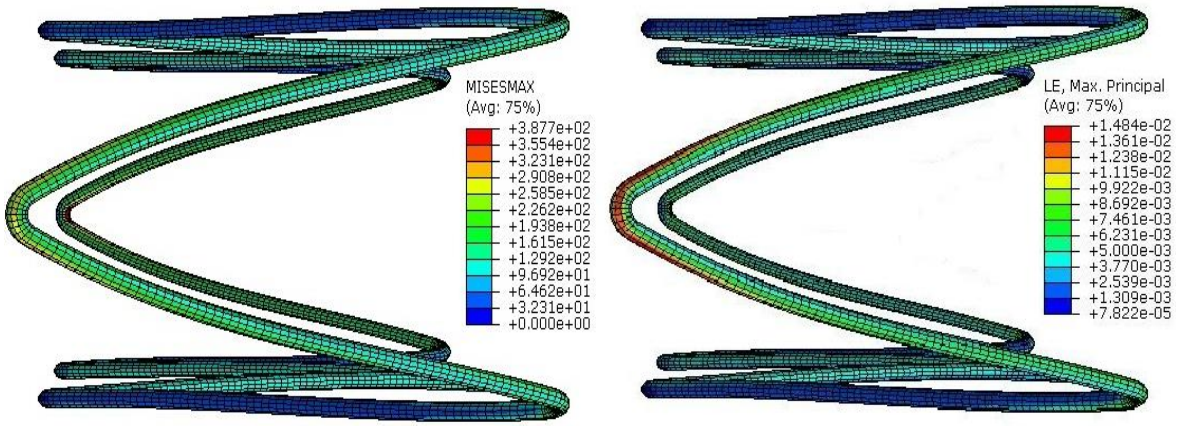

(a) (b)

Fig. 7. Result of 70% crushing of the TAA stent shown in **Fig. 1**: (a) MVMS, (b) MPS

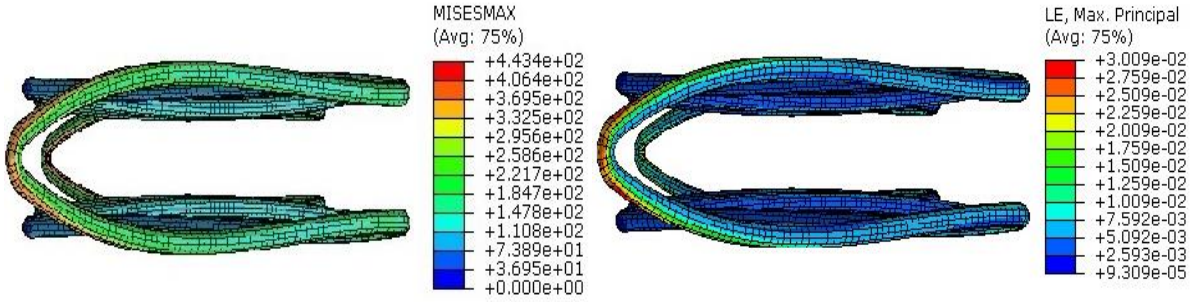

(a) (b)

Fig. 8. Result of 90% crushing of the TAA stent shown in **Fig. 1**: (a) MVMS, (b) MPS

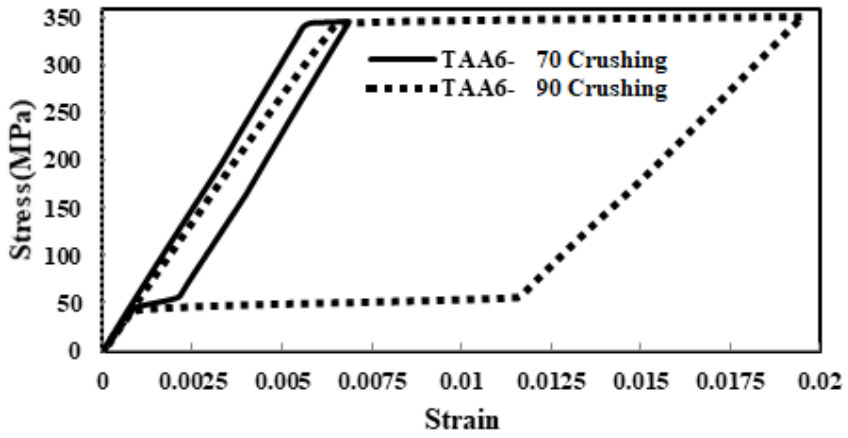

Fig. 9. Results of superelasticity behaviors plotted in 70% and 90% crushing on NiTi stent shown in **Fig 1.**

Biographies

Fardin Nematzadeh was born in Ardabil, Iran, in 1976. He received his B.S. degree in Materials Science and Engineering from Sahand University of Technology, Tabriz, Iran, in 1998, and his M.S. degree in Materials Science and Engineering from Sharif University of Technology, Tehran, Iran, in 2001, and his Ph.D. degree in Materials Science and Engineering from Sharif University of Technology and Material and Energy Center (MERC), Tehran, Iran in 2012.He has been joined the of Materials Engineering Department of Arak University as an assistant professor since 2012.His main research interests include: modeling and simulation in medical applications such as stent, shape memory alloys, biomaterials, Biomechanics and joining methods. He has published more than 50 papers in international journals and conferences. Currently, he is as a reviewer in a lot of technical valid journals such as Journal of Intelligent Material Systems and Structures, Journal of Biomedical Materials Research Part B Applied Biomaterials and Computer Methods in Biomechanics and Biomedical Engineering.

Hossein Mostaan was born in Ahvaz, Iran, in 1985. He received his B.S. degree in Materials Science and Engineering from Sharif University of Technology, Tehran, Iran, in 2007, and his M.S. degree in Materials Science and Engineering from Isfahan University of Technology, Isfahan, Iran, in 2010, and his Ph.D. degree in Materials Science and Engineering from Isfahan University of Technology, Isfahan, Iran in 2014.He has been joined the of Materials Engineering Department of Arak University as an assistant professor since 2014.His main research interests include: Mechanical and Physical of advanced Materials, Heat treatment of Metals, Welding Metallurgy and Powder Metallurgy, He has published more than 50 papers in international journals and conferences.